Fig. 1 shows the 'selected-area' point pattern from the $[11\bar{2}0]$ zone axis. This serves to show the rectangular cell dimensions 6·6 × 2·9 Å (*i.e.* $\sqrt{3}a/2 \times c$). The scale of the diffraction pattern is given by the carbon halo shown which corresponds to the *c*–*c* spacing of 2 Å. In the remaining figures the CBED–Kossel pattern (wide-angle convergent beam) and apertured convergent-beam patterns display the relevant symmetry elements, as follows:

1. The $[11\bar{2}0]$ zone-axis pattern of Fig. 2 shows the $2m$ symmetry of the projection. Note the $000l$, $l = 2n$ absences indicated by the dark band through the 0001 position.

2. Fig. 3(*a*) and (*b*) shows the patterns obtained from thin and thick crystals when the incident cone of electrons is parallel to the $\{000l\}$ planes but tilted several degrees to the $[11\bar{2}0]$ zone axis. This tilting increases the sensitivity of the pattern to any deviation from an [0001] mirror symmetry, by greatly increasing the zone of visible reflexions. In particular, the large tilt and large incident-cone semi-angle used for Fig. 3(*b*) bring up very many sharp defect lines within and around the direct (0000) beam. With these data we can verify the mirror plane in question (*i.e.* the mirror plane specific to $P6_3/m$ and absent from $P6_3$) to a high accuracy; certainly deviations of the order reported by Grun (1977) can be ruled out by this direct observation.

3. Fig. 4, taken with a tilt along the second axis, *i.e.* with the incident cone parallel to the $\{h\bar{h}00\}$ planes, shows the projective symmetry of the twofold screw axis. The absence of intensity at the 0001 position is in agreement with the twofold screw operator.

4. The wide-angle convergent-beam pattern of Fig. 5 which was taken at the $[11\bar{2}0]$ zone-axis setting has low contrast but an approximate $2m$ symmetry (the symmetry of the projection) can be seen. However, upon closer examination only the symmetry across the $[0001]^*$ line is exact.

Across the $[1\bar{1}00]^*$ axis a break in the symmetry (indicated on the figure) is in agreement with the well-known three-dimensional character of fast-electron-interaction crystal potential, and with the fact that its origin is not a mirror plane but the *projective* symmetry of a diad axis.

Conclusion

The above examination of β-Si_3N_4 shows accurate agreement with the $P6_3/m$ space group.

This work was supported by NSF Regional Facilities Instrumentation Grant No. CHE-7916098.

References

BORGEN, O. & SEIP, H. M. (1961). *Acta Chem. Scand.* **15**, 1789.

GOODMAN, P. (1980). *Convergent Beam Diffraction.* Proc. SEM Conference, Chicago. To be published.

GRUN, R. (1977). *Fortschr. Mineral.* **55**, 38–39.

HARDIE, D. & JACK, K. H. (1957). *Nature* (*London*), **180**, 332–333.

KATO, K., INOUE, Z., KIJIMA, K., KAWADA, I. & TANAKA, H. (1975). *J. Am. Ceram. Soc.* **58**, 90–91.

RUDDLESDEN, S. N. & POPPER, P. (1958). *Acta Cryst.* **11**, 465–468.

WILD, S., GRIEVESON, P. & JACK, K. H. (1972). *Spec. Ceram.* **5**, 385–393.

Acta Cryst. (1980). B**36**, 2893–2897

The Structure of Cs_3CoCl_5 at 295 K: A Neutron Diffraction Study

BY GEOFFREY A. WILLIAMS* AND BRIAN N. FIGGIS

School of Chemistry, The University of Western Australia, Nedlands, Western Australia 6009, *Australia*

AND FRANK H. MOORE

Australian Institute of Nuclear Science and Engineering, Sutherland, NSW 2232, *Australia*

(*Received* 8 *May* 1980; *accepted* 27 *June* 1980)

Abstract

The crystal structure of Cs_3CoCl_5 [tetragonal, $I4/mcm$, $a = 9{\cdot}2315$ (15), $c = 14{\cdot}5535$ (24) Å, $U = 1240{\cdot}3$ Å^3, $Z = 4$] has been determined at 295 K by the use of high-accuracy single-crystal neutron diffraction data. Automatic diffractometry has provided Bragg intensities for 490 independent reflections with $0 < \sin\theta/\lambda \leq 0{\cdot}690$ Å^{-1}, after equivalent reflections had been averaged. The structure was refined by full-matrix least-squares methods to R 0·023 and χ 1·454. Thermal-vibration parameters have been accurately

---

* Present address: Australian Radiation Laboratory, Lower Plenty Road, Yallambie, Victoria 3085, Australia.

0567-7408/80/122893-05$01.00

determined for all atoms, within an uncertainty in the estimated effects of thermal-diffuse scattering. The Co—Cl bond length in the $[CoCl_4]^{2-}$ ion is 2·2652 (3) Å (uncorrected) and 2·2754 (3) Å (corrected for rigid-body libration effects). The Cl—Co—Cl angles of the distorted tetrahedral Co environment are 106·97 (1) and 110·74 (1)°. The neutron scattering lengths of Cs and Co were found, by least-squares refinement, to be 5·38 (2) and 2·57 (3) fm respectively.

Introduction

The compound Cs_3CoCl_5 contains the $[CoCl_4]^{2-}$ anion as a tetragonally distorted tetrahedron. The simple chemical composition and high crystal symmetry have motivated a large number of studies of the physical properties of this compound (Figgis, Mason, Smith & Williams, 1980; and references therein). As well as these significant properties, a number of other features have influenced our choice of this compound for detailed studies of the valence-electron distribution and ligand—metal bonding by a variety of diffraction techniques.

The compound is paramagnetic at 4·2 K with three unpaired electrons. Furthermore, the $[CoCl_4]^{2-}$ tetrahedra are essentially magnetically isolated. These properties make Cs_3CoCl_5 ideally suited to a determination of the spin-density distribution by the technique of polarized neutron diffraction (Figgis, Mason, Smith & Williams, 1979). Such an experiment has been performed (Figgis, Reynolds, Williams, Mason, Smith & Varghese, 1980), and the results have been interpreted in terms of a chemically-based molecular-orbital description of the $[CoCl_4]^{2-}$ ion (Figgis, Reynolds & Williams, 1980). In short, it was determined that significant spin density was delocalized off the Co atom and onto the Cl ligands as well as into the Co—Cl overlap regions.

It is an attractive proposition to complement the spin-density studies by a charge-density analysis using X-ray diffraction data of high accuracy. Such a study is difficult because of the relatively high contribution of the Cs and Co core electrons to the scattering in general. However, the high site symmetries of most of the atoms in Cs_3CoCl_5 mean that some classes of reflections do not contain contributions from the electron density centred on certain of the atoms. This facilitates such a study of the valence-electron distribution, as will an independent determination of the thermal-vibration parameters of the atoms by a neutron diffraction experiment. High-accuracy X-ray diffraction data at 295 K have already been obtained for Cs_3CoCl_5 (Reynolds, Figgis & White, 1981), and it is primarily to aid in the separation of asphericity in the charge densities due to bonding and thermal effects in this analysis that the present neutron diffraction study of Cs_3CoCl_5 at 295 K has been undertaken.

The crystal structure of Cs_3CoCl_5 has been determined at room temperature with increasing accuracy by X-ray diffraction (Powell & Wells, 1935; Figgis, Gerloch & Mason, 1964; Reynolds, Figgis & White, 1981). As a corollary to the 4·2 K polarized neutron diffraction studies described above, the structure has also been determined at 4·2 K by neutron diffraction (Figgis, Mason, Smith & Williams, 1980). X-ray and neutron diffraction studies of Cs_3CoCl_5 are also anticipated at 100 K. The present 295 K neutron diffraction analysis therefore adds to the known temperature dependencies of the structural parameters, which may one day be used for a detailed 'molecular mechanics' calculation of the anionic distortions in relation to the intermolecular environment of the $[CoCl_4]^{2-}$ ion in Cs_3CoCl_5.

Experimental

The first crystal of Cs_3CoCl_5 chosen for study showed evidence of twinning. A second crystal was therefore selected, for which this was not a problem. The dimensions of this crystal were 4·5 × 4·0 × 2·8 mm, corresponding to the perpendicular distances between the well-developed $\{1\bar{1}0\}$, $\{001\}$, and $\{110\}$ crystal faces respectively. Neutron diffraction intensity data were obtained at 295 K and λ 1·241 Å on the '2TANB' four-circle diffractometer at the HIFAR reactor, Lucas Heights.

The space group was known to be $I4/mcm$ from previous studies, and the 295 K unit-cell parameters of $a = 9{\cdot}2315\,(15)$ and $c = 14{\cdot}5535\,(24)$ Å, obtained from a least-squares refinement of the setting angles of a number of Bragg reflections determined by X-ray diffractometry (Reynolds, Figgis & White, 1981), were used. Intensity data were collected by use of an ω–2θ scan during two reactor cycles, within the diffractometer limit $\sin\theta/\lambda \leq 0{\cdot}690$ Å^{-1}. A large number of the 16 possible equivalents were collected for most reflections. A total of 2926 reflections were measured, of which 2524 were distinct, allowed equivalents.

Small systematic fluctuations in the intensity of a standard reflection (404) were accurately determined by the 'Cumulative Sum' method (Moore & Colyvas, 1980) and the data were scaled accordingly. The maximum overall fluctuation in the intensity of the standard reflection was 3·3%. Integrated intensities were corrected for absorption [Cs_3CoCl_5, $\mu = 0{\cdot}0586$ mm^{-1} at 295 K, λ 1·241 Å (*International Tables for X-ray Crystallography*, 1968)] and for Lorentz effects. The transmission factor varied between 0·803 and 0·857. Distinct equivalent reflections were combined, yielding 490 unique non-equivalent observations. The agreement index $\sum \mathrm{Average}(|I - I_{av}|)/\sum |I_{av}|$ was 0·0206 for this process, where I is the intensity of a distinct equivalence, the summations are over all unique observations, and $I_{\rm av}$ is the relevant mean intensity of a unique observation.

The standard deviation in each $F^2_{\rm av}$, $\sigma(F^2_{\rm av})$, was taken as that determined either from counting statistics or from the deviations of the individual equivalences from their mean, whichever was the greater. Eight systematically absent reflections ($h0l$ with $l = 2n + 1$), and their equivalences, were also measured. These were all found to have $F^2_{\rm av} \geq 0{\cdot}0$, although several other reflections had small negative $F^2_{\rm av}$ values. The mean F^2 value for all eight systematic absences was 0·07, with a standard deviation of 0·08 for an individual data point, on a scale where the most intense reflection (440) had an F^2 value of 121·79. There was no indication of any systematic variation of this 'forbidden' intensity with $\sin\theta/\lambda$. This small 'forbidden' intensity is attributed to multiple scattering, and its effect is so small that it could almost certainly be neglected. However, we have chosen to correct the F^2 and $\sigma(F^2)$ values for a small general background of multiply scattered intensity (Le Page & Gabe, 1979). For each unique reflection, $F^2_o = F^2_{\rm av} - 0{\cdot}07$ and $\sigma(F^2_o) = [\sigma^2(F^2_{\rm av}) + (0{\cdot}08)^2]^{1/2}$.

Refinement

Starting parameters were obtained from the 295 K X-ray diffraction analysis of the Cs_3CoCl_5 structure (Reynolds, Figgis & White, 1981). The program *CRYLSQ* (Stewart, 1976) was used for the full-matrix least-squares refinements. The function minimized was $\sum w(F^2_o - F^2_c)^2$, where $w = 1/\sigma^2(F^2_o)$ is the weight assigned to the F^2_o values. Refinement (490 observations, 20 variables including scale, 3 positional and 13 anisotropic thermal parameters, Co and Cs scattering lengths, and an isotropic extinction coefficient) converged with $R = \sum |F^2_o - F^2_c|/\sum F^2_o = 0{\cdot}023$ and a goodness-of-fit index $\chi = [\sum w(F^2_o - F^2_c)^2/(n - v)]^{1/2} = 1{\cdot}454$, where n and v are numbers of observations and variables respectively. The maximum parameter shift-to-error ratio at convergence was 0·06:1. A final difference synthesis was featureless, the maximum and minimum densities being 0·21 and −0·32 fm. The extinction coefficient refined to $5{\cdot}30\,(5) \times 10^3$ (Larson, 1967), using the individual transmission path length for each reflection, averaged over all measured equivalences. The neutron scattering lengths of Cs and Co were refined to 5·38 (2) and 2·57 (3) fm respectively, with the scattering length of Cl fixed at 9·58 fm (*International Tables for X-ray Crystallography*, 1974).*

Table 1. *Final atomic positional coordinates and thermal parameters for* Cs_3CoCl_5

Only the variable parameters are presented. The atoms are at the positions Co $(0,\frac{1}{2},\frac{1}{4})$; Cs(1) $(0,0,\frac{1}{4})$; Cs(2) $(x, \frac{1}{2} + x, 0)$; Cl(1) (0,0,0); Cl(2) $(x, \frac{1}{2} + x, z)$. Anisotropic thermal parameters are defined by $T = \exp[-2\pi^2(h^2a^{*2}U_{11} + k^2b^{*2}U_{22} + l^2c^{*2}U_{33} + 2hka^*b^*U_{12} + 2hla^*c^*U_{13} + 2klb^*c^*U_{23})]$. U tensors are in Å². All U values not listed below are zero, with the exceptions $U_{22} = U_{11}$ for all atoms and $U_{23} = U_{13}$ for Cl(2).

Variable	Refinement 1 (all data)	Refinement 2 ($\sin\theta/\lambda \leq 0{\cdot}5$ Å^{-1})	Refinement 3 ($\sin\theta/\lambda > 0{\cdot}5$ Å^{-1})
x[Cs(2)]	0·66565 (5)	0·66575 (8)	0·66561 (5)
x[Cl(2)]	0·13945 (2)	0·13945 (4)	0·13943 (3)
z[Cl(2)]	0·15738 (2)	0·15750 (3)	0·15731 (2)
U_{11}[Co]	0·0267 (6)	0·0284 (11)	0·0273 (4)
U_{33}[Co]	0·0193 (8)	0·0202 (17)	0·0198 (6)
U_{11}[Cs(1)]	0·0403 (3)	0·0407 (6)	0·0411 (3)
U_{33}[Cs(1)]	0·0341 (5)	0·0334 (10)	0·0346 (5)
U_{11}[Cs(2)]	0·0249 (2)	0·0254 (4)	0·0255 (2)
U_{33}[Cs(2)]	0·0324 (3)	0·0314 (6)	0·0332 (3)
U_{12}[Cs(2)]	−0·0014 (2)	−0·0013 (5)	−0·0014 (2)
U_{11}[Cl(1)]	0·0271 (2)	0·0275 (3)	0·0277 (2)
U_{33}[Cl(1)]	0·0428 (3)	0·0421 (6)	0·0436 (3)
U_{11}[Cl(2)]	0·0403 (1)	0·0408 (3)	0·0410 (2)
U_{33}[Cl(2)]	0·0347 (1)	0·0339 (3)	0·0355 (2)
U_{12}[Cl(2)]	−0·0117 (1)	−0·0118 (2)	−0·0118 (1)
U_{13}[Cl(2)]	0·0065 (1)	0·0066 (2)	0·0064 (1)

A possibly significant error remaining, not corrected in the data or included in the scattering model, is the effect of thermal diffuse scattering (TDS) on the thermal-vibration parameters. To determine the $\sin\theta/\lambda$ dependence of the effects of TDS, two refinements were performed using different portions of the data. In these refinements, scattering lengths and the extinction coefficient were fixed at their refined positions above.

Refinement (194 observations with $0 < \sin\theta/\lambda \leq 0{\cdot}5$ Å^{-1}, 17 variables) converged with R 0·020 and χ 1·553. The maximum shift-to-error ratio at convergence was 0·09:1. For the higher-angle data, refinement (296 observations with $0{\cdot}5 < \sin\theta/\lambda \leq 0{\cdot}69$ Å^{-1}, 17 variables) converged with R 0·025 and χ 1·239. The maximum shift-to-error ratio at convergence was 0·04:1. The atomic positional and thermal parameters from both these refinements, together with those from the refinement employing all data, are presented in Table 1.

Finally, as a check on the effects on the atomic parameters of possible shortcomings in the isotropic model used to correct for extinction (Larson, 1967), a refinement was performed omitting all data seriously affected by extinction. All observations for which the extinction correction factor for F^2 was <0·9 were omitted, and refinement (452 observations, 20 variables) converged with R 0·024 and χ 1·283. The maximum shift-to-error ratio at convergence was 0·07:1. There was no significant change in any of the

---

* A list of structure factors has been deposited with the British Library Lending Division as Supplementary Publication No. SUP 35522 (5 pp.). Copies may be obtained through The Executive Secretary, International Union of Crystallography, 5 Abbey Square, Chester CH1 2HU, England.

structural parameters from the values obtained by refinement employing all data. The extinction coefficient refined to the value 4·94 (19) × 10^3.

Initial data processing used the Lucas Heights Single Crystal Data Reduction System on an IBM System 370 computer. Structure refinement used the XRAY76 program system (Stewart, 1976) implemented on a Perkin Elmer 8/32 computer at the Crystallography Centre of the University of Western Australia.

Results and discussion

An *ORTEP* view (Johnson, 1965) of the structure of Cs_3CoCl_5 is shown in Fig. 1. The unit-cell dimensions of Cs_3CoCl_5, together with the bond lengths and angles in the $[CoCl_4]^{2-}$ ion, are presented in Table 2, along with the 295 K X-ray values for comparison. Interatomic distances at 295 K, from the present neutron analysis of the Cs_3CoCl_5 structure, are given in Table 3.

Table 2. *Unit cell, bond lengths and angles in* Cs_3CoCl_5 *at* 295 K

	A	*B*	*C*	*D*
a (Å)	9·2315 (15)	–	–	–
c (Å)	14·5535 (24)	–	–	–
U (Å^3)	1240·26	–	–	–
Co—Cl (Å)	2·266 (1)	2·277 (1)	2·2652 (3)	2·2754 (3)
Cl—Co—Cl (°)	107·13 (4)	107·09 (4)	106·97 (1)	106·92 (1)
	110·66 (3)	110·67 (3)	110·74 (1)	110·76 (1)

(*A*) Values taken from the X-ray study of Reynolds, Figgis & White (1981).
(*B*) Bond length and angles of (*A*) corrected for rigid-body libration effects by the **TLS** method of Schomaker & Trueblood (1968).
(*C*) Values from the present neutron analysis.
(*D*) Bond length and angles of (*C*) corrected for rigid-body libration effects as in (*B*). Corrected coordinates for Cl(2) are *x* 0·14003 (2), *z* 0·15692 (2).

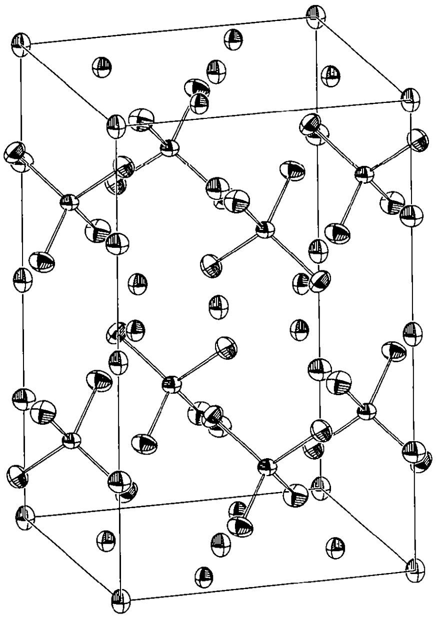

Fig. 1. An *ORTEP* drawing of the Cs_3CoCl_5 unit cell. Thermal parameters, uncorrected for TDS effects, have been used in representing the thermal ellipsoids at the 60% probability level.

Table 3. *Interatomic contacts* (Å) *less than* 4 Å *in* Cs_3CoCl_5 *at* 295 K

Cs(1)···Cl(1) ×2	3·6384 (6)	Cl(2)···Co	2·2652 (3)
···Cl(2) ×8	3·8148 (5)	···Cs(1) ×2	3·8148 (5)
Cs(2)···Cl(1) ×2	3·4446 (6)	···Cs(2)	3·4236 (5)
···Cl(2) ×2	3·4236 (5)	···Cs(2) ×2	3·6383 (6)
···Cl(2) ×4	3·6383 (6)	···Cl(2)	3·6410 (5)
Cl(1)···Cs(1) ×2	3·6384 (6)	···Cl(2) ×2	3·7277 (6)
···Cs(2) ×4	3·4446 (6)	···Cl(2)	3·9497 (5)

The atomic coordinates from the present neutron diffraction study of Cs_3CoCl_5 are believed to specify the crystal structure more accurately than has been done before. This is not only because of the quality of the intensity data employed in the analysis, but also because the neutron diffraction experiment yields the true nuclear positions, unlike refinements based on X-ray diffraction data which give the atomic position at the centroid of the electron density. Similarly, if TDS can be neglected, the thermal-vibration parameters obtained from the neutron diffraction analysis represent the true thermal motion of the nucleus, and are uncorrelated with any asphericity in the valence electron density. For the $\sin\theta/\lambda$ limit of the data (0·690 Å^{-1}), the effects of anharmonicity in the thermal motion are insignificant. A comparison with the thermal-vibration parameters, obtained from a refinement of the Cs_3CoCl_5 structure employing extensive X-ray data, will be presented elsewhere (Reynolds, Figgis & White, 1981).

The results of the high- and low-angle refinements (Table 1) do not indicate any significant systematic variations in the thermal parameters. Hence we can assume that TDS effects, if present, are essentially constant over the $\sin\theta/\lambda$ range of the data. As Cs_3CoCl_5 is a 'soft' material, at the experimental wavelength of 1·241 Å, TDS is almost certainly significant (Willis & Pryor, 1975). An approximate spherical correction for the effects of TDS can be made using the experimental conditions and by estimating, rather crudely, the elastic constants from the infrared spectrum of Cs_3CoCl_5 (Brown-Acquaye & Lane, 1977). To first order we obtain a correction of 0·025 ± 0·009 Å^2 which must be added to the refined values (Table 1) of the diagonal elements of U_{ij}.

GAW thanks the Australian Institute of Nuclear Science and Engineering for a Research Fellowship. We thank Dr P. A. Reynolds for helpful discussions.

References

Brown-Acquaye, H. A. & Lane, A. P. (1977). *J. Inorg. Nucl. Chem.* **39**, 2277–2282.

FIGGIS, B. N., GERLOCH, M. & MASON, R. (1964). *Acta Cryst.* **17**, 506–508.

FIGGIS, B. N., MASON, R., SMITH, A. R. P. & WILLIAMS, G. A. (1979). *J. Am. Chem. Soc.* **101**, 3673–3675.

FIGGIS, B. N., MASON, R., SMITH, A. R. P. & WILLIAMS, G. A. (1980). *Acta Cryst.* B**36**, 509–512.

FIGGIS, B. N., REYNOLDS, P. A. & WILLIAMS, G. A. (1980). *J. Chem. Soc. Dalton Trans.* In the press.

FIGGIS, B. N., REYNOLDS, P. A., WILLIAMS, G. A., MASON, R., SMITH, A. R. P. & VARGHESE, J. N. (1980). *J. Chem. Soc. Dalton Trans.* In the press.

International Tables for X-ray Crystallography (1968). Vol. III, pp. 197–199. Birmingham: Kynoch Press.

International Tables for X-ray Crystallography (1974). Vol. IV, pp. 270–271. Birmingham: Kynoch Press.

JOHNSON, C. K. (1965). *ORTEP*. Report ORNL-3794. Oak Ridge National Laboratory, Tennessee.

LARSON, A. C. (1967). *Acta Cryst.* **23**, 664–665.

LE PAGE, Y. & GABE, E. J. (1979). *Acta Cryst.* A**35**, 73–78.

MOORE, F. H. & COLYVAS, K. (1980). Unpublished data.

POWELL, H. M. & WELLS, A. F. (1935). *J. Chem. Soc.* pp. 359–362.

REYNOLDS, P. A., FIGGIS, B. N. & WHITE, A. H. (1981). *Acta Cryst.* In the press.

SCHOMAKER, V. & TRUEBLOOD, K. N. (1968). *Acta Cryst.* B**24**, 63–76.

STEWART, J. M. (1976). The XRAY 76 system. Tech. Rep. TR-446. Computer Science Center, Univ. of Maryland, College Park, Maryland.

WILLIS, B. T. M. & PRYOR, A. W. (1975). *Thermal Vibrations in Crystallography*, pp. 232–241. Cambridge Univ. Press.

Acta Cryst. (1980). B36, 2897–2902

The Structure of $Ba_xTi_{8-2x}Ga_{10+2x}O_{31}$

BY L. A. BURSILL*

Department of Physical Chemistry, Lensfield Road, Cambridge CB2 1EP, England

(*Received* 4 *December* 1979; *accepted* 21 *July* 1980)

Abstract

The crystal structure of $Ba_xTi_{8-2x}Ga_{10+2x}O_{31}$ is studied by high-resolution (3 Å) electron microscopy. The tunnel structure contains elements of the hollandite, rutile and β-gallia structure types, intergrown coherently to produce a tetragonal unit cell with $a_1 = a_2 = 19{\cdot}1$ and $c = 2{\cdot}96$ Å. Computer simulation of the images shows that a structural model, derived by intuitive interpretation of an image recorded near the Scherzer defocus condition, gives a good image match with experimental images, provided full N-beam multislice techniques are employed.

1. Introduction

The structural relationships between hollandite, rutile and a number of other titanate structures suggested (Bursill, 1979*a*) that hollandite-type tunnels could be produced at orthogonal intersections of $\{210\}\ \langle\frac{1}{2}\frac{1}{4}\frac{1}{2}\rangle$ crystallographic shear planes in rutile. Examples of 25 distinct defect intersection structures were found in a study of Mg- and Ga-doped rutiles (Bursill, 1979*b*). Now the structure building element common to both hollandite and β-Ga_2O_3 is a double-string of edge-shared $[MO_6]$ octahedra parallel to $c_{\rm holl}$ or b_β (*cf.* Figs. 1*b* and 4*b* in Bursill, 1979*a*) and it was therefore predicted that Ba-hollandites containing Ga^{3+} in the framework would be relatively more stable than those containing other trivalent cations, *e.g.* Mn, Ti, Al, which do not adopt the β-Ga_2O_3-type structure. We therefore attempted to prepare hollandites having formulae $Ba_xTi_{8-2x}Ga_{2x}O_{16}$ with $x < 0{\cdot}5$. A sample of mean stoichiometry $x = 0{\cdot}5$ was found to contain two phases. The major phase was a hollandite with $x = 0{\cdot}8$ which exhibited incommensurate superlattice ordering of Ba^{2+} ions along the hollandite tunnels (Bursill, 1979*c*; Bursill & Grzinic, 1980). The minor component exhibited a 19·1 × 19·1 Å tetragonal unit cell and this unknown structure became the subject of this paper. It provided a good test object for a goniometer developed for use in objective-lens pole pieces having spherical-aberration coefficient $C_s = 0{\cdot}7$ mm (Bursill, Spargo, Wentworth & Wood, 1979).

2. Experimental

Weighed amounts of finely powdered Ga_2O_3, TiO_2 and $BaCO_3$ (Koch-Light, 4N) having overall stoichiometry

---

* On leave from: School of Physics, The University of Melbourne, Parkville, Victoria 3052, Australia.

0567-7408/80/122897-06$01.00